

Mechanism of barotaxis in marine zooplankton

Luis Alberto Bezares Calderón^{1,*}, Réza Shahidi^{1,2}, Gáspár Jékely^{1,3,*}

¹Living Systems Institute, University of Exeter, Stocker road, Exeter, EX4

² Electron Microscopy Core Facility (EMCF), University of Heidelberg, 69120 Heidelberg, Germany

³Heidelberg University, Centre for Organismal Studies (COS), 69120 Heidelberg, Germany

*Correspondence: l.a.bezares-calderon @ exeter.ac.uk, gaspar.jekely @ cos.uni-heidelberg.de

1 Table of contents

2 Abstract

3 Hydrostatic pressure is a dominant environmental cue for vertically migrating marine organisms but the
4 physiological mechanisms of responding to pressure changes remain unclear. Here we uncovered
5 the cellular and circuit bases of a barokinetic response in the planktonic larva of the marine annelid
6 *Platynereis dumerilii*. Increased pressure induced a rapid, graded and adapting upward swimming re-
7 sponse due to the faster beating of cilia in the head multiciliary band. By calcium imaging, we found
8 that brain ciliary photoreceptors showed a graded response to pressure changes. The photoreceptors in
9 animals mutant for *ciliary opsin-1* had a smaller sensory compartment and mutant larvae showed dimin-
10 ished pressure responses. The ciliary photoreceptors synaptically connect to the head multiciliary band
11 via serotonergic motoneurons. Genetic inhibition of the serotonergic cells blocked pressure-dependent
12 increases in ciliary beating. We conclude that ciliary photoreceptors function as pressure sensors and
13 activate ciliary beating through serotonergic signalling during barokinesis.

14 #

15 Introduction

16 Hydrostatic pressure increases linearly with depth in the ocean and planktonic organisms can use it as a
17 depth cue, which is independent of light or the time of the day (Blaxter, 1978). Many marine invertebrate
18 animals have long been known to sense and respond to changes in pressure (Knight-Jones and Qasim,
19 1955; Rice, 1964). The response generally consists of an increase in locomotion (barokinesis) upon an
20 increase in pressure. Such responses could help planktonic animals retain their depth either in combi-
21 nation with, or independent of light cues (Forward et al., 1989). Changes in hydrostatic pressure may
22 additionally entrain tidal rhythms in marine animals (Akiyama, 2004; Morgan, 1965; Naylor and Williams,
23 1984).

24 Early studies on the barokinetic response in zooplankton have not revealed if the animals respond to relative or absolute changes in pressure. The kinematics and neuronal mechanisms of pressure responses
25 have also not been characterized in detail for any planktonic animal. The most familiar structures for
26 sensing changes in hydrostatic pressure are gas-filled compressible vesicles such as the swim bladder
27 in fish (Qutob, 1963). However, barokinetic responses are seen across many animals without any identifiable
28 gas-filled vesicles. What structures could mediate pressure sensing in these organisms? Thus far,
29 only a few alternative structures have been proposed for pressure sensation. In the statocyst of the adult
30 crab *Carcinus maenas*, millimeter-sized thread-hairs may act as a syringe plunger to sense pressure
31 (Fraser and Macdonald, 1994). In dogfish, which lack a swim bladder, hair cells in the vestibular organ
32 have been proposed to act as pressure detectors (Fraser and Shelmerdine, 2002). It is unknown which,
33 if any, of these two vastly different pressure sensing mechanisms—one based on volume changes in a
34 gas-filled vesicle and the other on deformation of sensory cilia—is used by the much smaller planktonic
35 animals.

36 To understand the behavioural and neuronal mechanisms of pressure responses in marine zooplankton,
37 we studied the planktonic ciliated larvae of the marine annelid *Platynereis dumerilii* (Özpolat et al., 2021). This larva uses ciliary beating to swim up and down in the water column to eventually settle on sea grass beds near coastal regions (Gambi et al., 1992). The sensory and neuronal bases of
38 light-guided (Gühmann et al., 2015; Randel et al., 2014; Verasztó et al., 2018) and mechanically-driven
39 behaviours (Bezares-Calderón et al., 2018) in *Platynereis* larvae have been dissected due to the experimental
40 tractability of this system. Its small size has allowed the entire reconstruction of the cellular and
41 synaptic wiring map of the three-day-old larva (Jasek et al., 2022; Jékely et al., 2024). Here we study
42 *Platynereis* larvae to understand the cellular and neuronal bases of pressure sensation in zooplankton.
43

44 **Results**

45 ***Platynereis* larvae respond to changes in hydrostatic pressure**

46 To determine whether *Platynereis* larvae respond to changes in hydrostatic pressure, we developed a custom behavioural chamber with precise pressure control. We subjected larvae to step changes in pressure and recorded their behaviour under near-infrared illumination (Figure 1A; see Materials and Methods). We used hydrocarbon-free compressed air to increase pressure in the chamber. We tested a range of pressure levels in randomized order from 3 mbar to 1000 mbar (1 mbar equals to 1 cm water depth) (Figure 1—figure supplement 1A). We focused on one- to three-day-old larvae corresponding to the early and late trophophore and neotrochophore stages. We used batches of > 100 larvae for each experiment. Both two-day-old and three-day-old larvae respond to pressure increase by swimming upwards faster and in straighter trajectories, as quantified by changes in average vertical displacement, swimming speed, the ratio of upward to downward trajectories (Figure 1B–C, Figure 1—figure supplement 1B–D; Video 1), and a straightness index (the net over total distance) (Figure 1—figure supplement 1E).

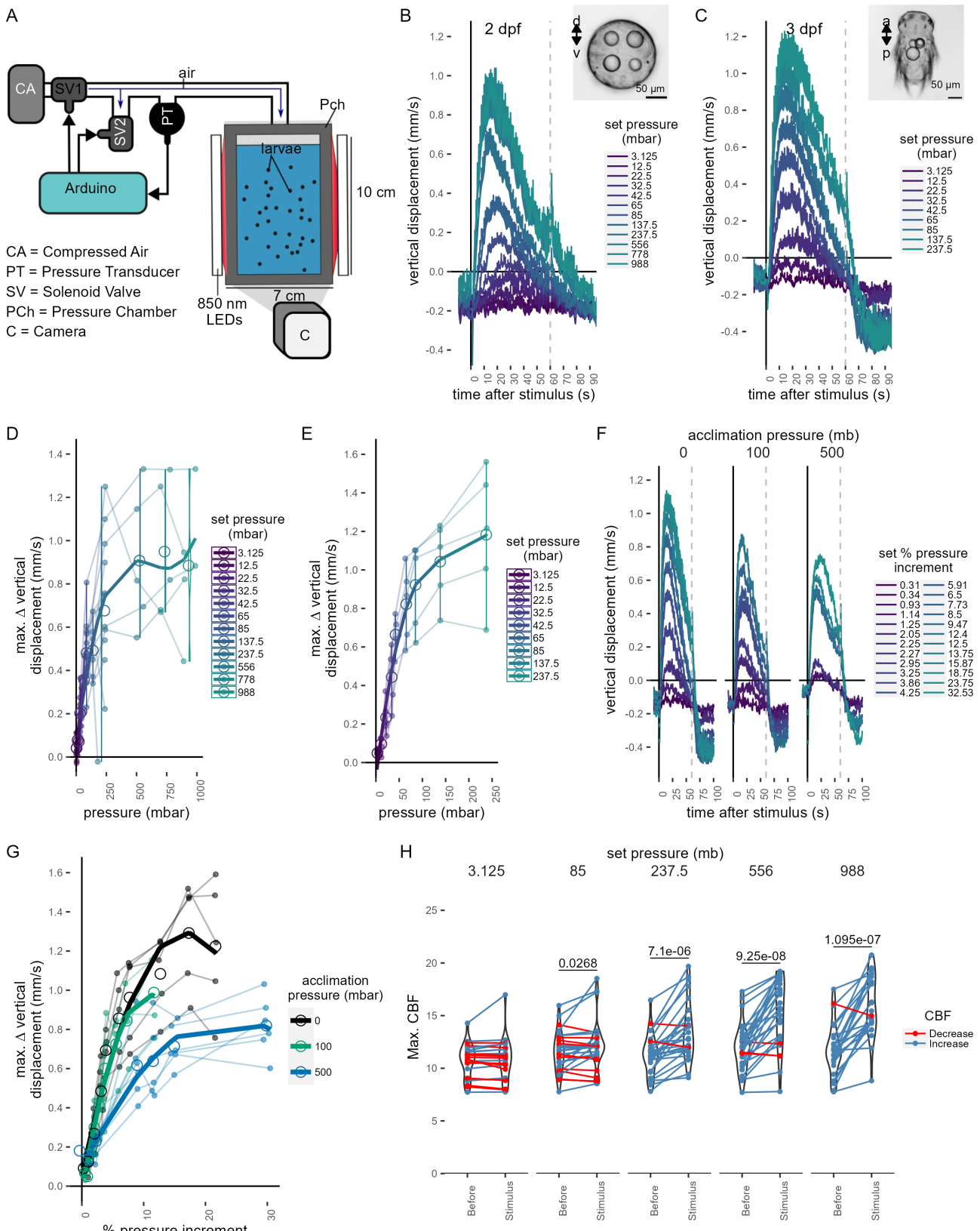


Fig. 1: Figure 1. Pressure response in *Platynereis* larvae. (A) Schematic of the behavioural setup used to stimulate larvae with controlled pressure levels. (B-C) Vertical displacement of (B) two-day-old and (C) three-day-old larvae (insets) as a function of time relative to different step increases in pressure. Dashed line at 60 s indicates the end of stimulation. Each data point is the average of 2 to 12 (B), or 4 to 5 (C) batches of larvae. (D-E) Maximum increase in relative vertical displacement of (D) two-day-old and (E) three-day-old larvae for each pressure level tested. Small filled circles represent individual data points, data points from the same batch are joined by lines. Larger open circles indicate the mean across all batches. (F) Vertical displacement of three-day-old larvae acclimated for ca. 10 min to either ambient

59 We used the maximal vertical displacement value (normalised to the mean displacement per trial prior to
60 stimulus presentation) to compare the magnitude of responses as a function of pressure change. In both
61 two- and three-day-old larvae the responses were graded: higher pressure levels led to higher maximal
62 vertical displacement (Figure 1D–E). Three-day-old larvae had a slightly lower sensitivity threshold (10-20
63 mbar) than two-day-old larvae (20-30 mbar) and their response plateaued at lower pressure levels than
64 that of two-day-old larvae (Figure 1B-E). One-day-old larvae did not show a detectable response to even
65 the largest pressure levels tested (Figure 1—figure supplement 2A–B). The straightness of trajectories
66 also increased with increasing pressure changes. This was due to narrower helical swimming paths
67 under pressure, visible in close-up videos (Video 2 & Video 3). Three-day-old larvae also showed a
68 diving response upon the release of pressure (Figure 1B–C, F; Figure 1—figure supplement 1C–D).
69 Two-day-old larvae stopped moving upwards when the stimulus ended, but did not show an active diving
70 response to pressure OFF.

71 To exclude the possibility that either the changes in the partial pressure of gases due to the use of
72 compressed air, or the mechanical wave associated to the inflow of air caused the upward swimming
73 behaviour, we also used a static column of water of different heights to change pressure levels (Figure 1—
74 figure supplement 2C). We observed the same dependence of vertical displacement on the magnitude
75 of pressure change in this setup (Figure 1—figure supplement 2D-E). Overall, our experiments uncov-
76 ered a graded, saturable and highly sensitive upward swimming ON response to increased pressure in
77 *Platynereis* larvae and a diving OFF response (in three-day-old larvae only).

78 ***Platynereis* larvae respond to relative changes of pressure**

79 Larvae may either detect absolute pressure levels, relative changes, or the rate at which pressure
80 changes (Morgan, 1984). To differentiate between these possibilities, we first exposed larvae to linear
81 increases of pressure with rates between 0.05 mbar s⁻¹ and 2.6 mbar s⁻¹ (Figure 1—figure supplement
82 3A). We used a 2nd-degree polynomial function for rate categories 0.3-0.7 mbar s⁻¹ (ANOVA, p = 6.5e-3)
83 and 0.9-1.3 mbar s⁻¹ (ANOVA, p= 5.8e-8), as it described the relationship between vertical displacement
84 and pressure more accurately than a simple linear model. The difference between a linear and a 2nd-
85 degree polynomial fit was not significant for rates > 1.3 mbar s⁻¹ (ANOVA, p~ 0.1). These results suggest
86 that larvae compensate for the increase in pressure by a corresponding increase in upward swimming
87 when rates of pressure increase are sufficiently high.

88 The linear response to a gradual increase in pressure suggests that larvae detect changes in pressure,
89 rather than absolute pressure levels. To directly address this, we acclimated three-day-old larvae for ca.
90 10 min to either 100 mbar or 500 mbar pressure above the atmospheric level. We then tested a range
91 of randomized step-increases in pressure levels (Figure 1—figure supplement 3D). After the acclimation
92 period, the distribution of larvae exposed to 100 mbar or 500 mbar was not different from the larvae kept
93 at ambient levels (two-sided Kolmogorov Smirnoff test, 0–100 mbar: p = 0.915, 0–500 mbar: p = 0.0863)
94 (Figure 1—figure supplement 3E–F). Upon step increase, larvae reacted with graded upward swimming
95 even if they were pre-exposed to 100 or 500 mbar (Figure 1F). The sensitivity decreased when larvae
96 were acclimated to 500 mbar (Figure 1G). When pressure was released at the end of the increase trials,
97 larvae pre-exposed to 500 mbar showed a downward displacement followed by an upward displacement

98 as soon as pressure was increased back to the corresponding basal level (Figure 1—figure supplement
99 3G). The downward displacement resembled the magnitude of the diving response we observed for
100 3-day-old larvae (Figure 1—figure supplement 3H).

101 Our experiments suggest that *Platynereis* larvae react to relative increases in pressure in a graded man-
102 ner proportional to the magnitude of the increase. The response is adaptable and occurs at very different
103 basal pressures (0 mbar or 500 mbar—corresponding to surface or 5 m of water depth). This hints at a
104 pressure-gauge mechanism to regulate swimming depth by compensating for vertical movements due
105 to down-welling currents (Genin et al., 2005), sinking (when cilia are arrested (Verasztó et al., 2017)) or
106 downward swimming (e.g., during UV-avoidance (Verasztó et al., 2018)).

107 **Ciliary beat frequency increases with pressure**

108 To understand the mechanism by which larvae regulate swimming in response to an increase in pressure,
109 we analysed the effect of pressure on ciliary beating in the prototroch—the main ciliary band that propels
110 swimming in two-day-old and three-day-old *Platynereis* larvae. Individual two-day-old larvae were teth-
111 ered to a glass cuvette from the posterior end with a non-toxic glue previously used in *Platynereis* larvae
112 (Bezares-Calderón et al., 2018). The cuvette was inserted into a custom-made pressure vessel placed
113 under a microscope. We applied 60-sec step increases in pressure in a randomized order and recorded
114 ciliary beating in effective darkness (Figure 1—figure supplement 4A, B).

115 The mean ciliary beat frequency increased as soon as a step change in pressure was applied, with
116 larger step changes showing more noticeable increases in beat frequency (Figure 1—figure supplement
117 4C, Video 4). The maximum ciliary beat frequency (max. CBF) during the stimulus period showed a
118 statistically significant increase for all but the lowest pressure steps tested relative to the period before
119 the onset of the stimulus (85 mb p = 0.046, 237.5 mb p = 2.08 E-05, 556 mb p = 8.35 E-07, 988 mb p = 7.8
120 E-07; one-tailed paired t-test with Bonferroni correction testing for an increase in CBF; Figure 1H). The
121 related relative measure of maximum percent change (max. Δ%CBF) also showed an increase under
122 pressure (Figure 1—figure supplement 4D). Overall, these data suggest that rapid upward swimming
123 under pressure is due to an increase in the beating frequency of prototroch cilia that is proportional to
124 the change in pressure.

125 **Brain ciliary photoreceptor cells show graded activation under increased pressure**

126 To identify the pressure-sensitive cells in *Platynereis* larvae, we developed an approach to couple imaging
127 of neuronal activity with pressure increases (Figure 2A). We injected fertilised eggs with mRNA encod-
128 ing the calcium indicator GCaMP6s (Chen et al., 2013)—an indirect reporter of neuronal activity—and
129 embedded injected larvae in low-melting agarose. Mounted larvae were introduced into a custom-built
130 microscopy chamber, where pressure could be increased using compressed air. To provide morpholog-
131 ical landmarks and to correct for Z-shifts during imaging, we co-injected larvae with an mRNA encoding
132 the membrane-tagged reporter palmitoylated tdTomato.

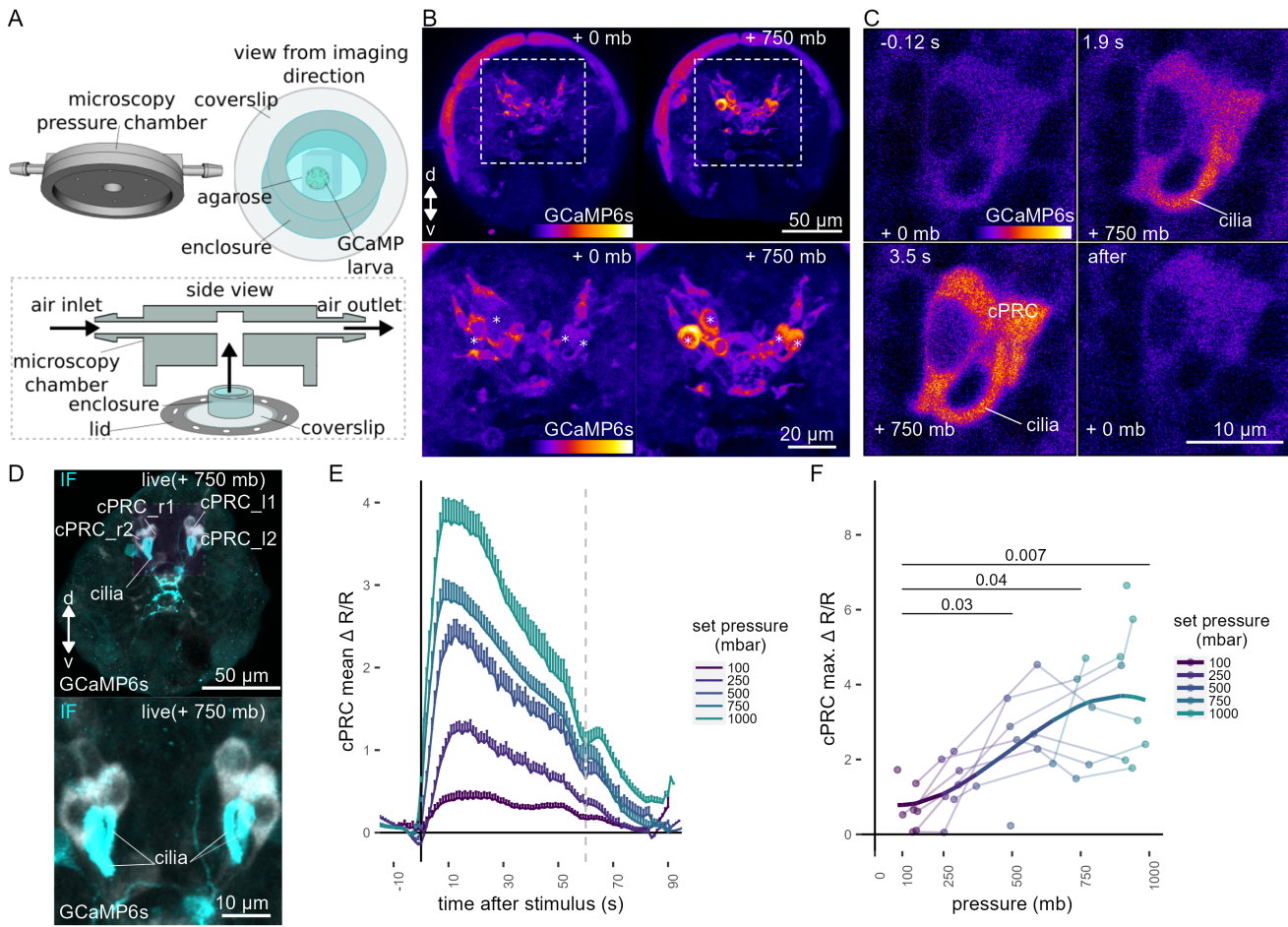


Fig. 2: Figure 2. Ca^{2+} imaging of *Platynereis* larvae during pressure increases. (A) Ca^{2+} imaging preparation to analyse neuronal activation upon pressure stimulation. Left: side view of the 3D model of the microscopy pressure chamber. Right: Larvae embedded in agarose are placed on a round coverslip. An enclosure around the embedded larva serves to keep it under water. Bottom: the enclosed larva on the coverslip is inserted in the central hole of the chamber. A screwable lid secures the coverslip to the chamber and prevents air leaks. Pressure is increased with compressed air entering from one of the inlets. (B, top) Maximum intensity projection of a two-day-old larva injected with GCaMP6s mRNA acquired before (left) or during (right) the pressure stimulus. (B, bottom) Enlarged views of the corresponding regions highlighted with dashed squares in the top panels. Asterisks mark the position of cell nuclei of the four cells activated by pressure. (C) Still images of a cPRC acquired at different time points relative to increase in pressure ($t = 0$, Video 5). The time points are indicated on the upper left of each panel. Pressure level is also indicated. (D) Maximum intensity projection of a GCaMP6s Z-stack during raised pressure (white channel) and of a Z-stack of the same larva after immunofluorescence (IF) with NIT-GC2, a marker for cPRC cilia (Jokura et al., 2023), and for serotonin (cyan channel). Anterior view in B–D. (E) Mean $\Delta R/R$ in cPRC_I1 across different step increases in pressure as a function of time of stimulation. Dashed line at 60 s marks the end of stimulus. $N = 8$ larvae. (F) Max. $\Delta R/R$ in cPRC_I1 as a function of pressure level. Data points from the same larva are joined by lines. Regression line fitting the data is also shown. One-tailed unpaired t-test with Bonferroni correction testing for an increase in Max. $\Delta R/R$ with pressure. p -values < 0.05 are shown. Figure 2—source data 1 (E–F).

133 By imaging the entire larva before and during the pressure stimulus, we found a group of four cells
 134 in the dorsomedial brain that showed consistent increases in GCaMP6s fluorescence when pressure

increased (Figure 2B; Figure 2—figure supplement 1). Time-lapse recordings of these cells revealed that they had prominent cilia, which become visible by the increase in GCaMP6s signal during pressure increase (Figure 2C, Figure 2—Supplement Video 1). The position, number, size and morphology of these cells closely matched to that of the previously described brain ciliary photoreceptor cells (cPRCs) (Arendt et al., 2004; Tsukamoto et al., 2017; Verasztó et al., 2018). Immunostaining of the same larvae that were used for Ca^{2+} imaging with an antibody raised against NIT-GC2, a marker of cPRC cilia (Jokura et al., 2023), followed by image registration directly confirmed that the four cells activated under pressure were the cPRCs (Figure 2D).

To characterise the response of cPRCs to pressure, we applied a randomised set of pressure increases (Figure 2—figure supplement 2A) to two-day-old larvae expressing GCaMP6s while recording fluorescence changes in the four cPRCs. All four cPRCs responded to the pressure levels tested (Figure 2E; Figure 2—figure supplement 2B–C). This response—like that observed at the behavioural level—was graded and increased proportionally to the pressure change (Figure 2E–2F; Figure 2—figure supplement 2B–C, 2E). The difference in the response between pressure levels was statistically significant for some of the cPRCs (Figure 2F; Figure 2—figure supplement 2C). The calcium signal also decreased rapidly after stimulus onset. Therefore, cPRCs may be able to directly encode the intensity of the stimulation in their activity, reflected in their internal Ca^{2+} levels, and adapt to pressure levels. Their unique sensory morphology and pressure-induced Ca^{2+} dynamics make the cPRCs candidate pressure receptors.

An additional unpaired sensory cell on the dorsal side was also activated in some of the trials (Figure 2—figure supplement 1, green asterisk). We refer to this cell here as $\text{SN}^{\text{d1_unp}}$ (by position and morphology it corresponds to the neurosecretory cell $\text{SN}^{\text{YFa}+}$ (Williams et al., 2017)). At 750 mb, this cell responded by a transient but robust increase at stimulation onset, but $\Delta R/R$ dropped to basal values before the end of the stimulus, unlike the cPRC response (Figure 2—figure supplement 2D). $\text{SN}^{\text{d1_unp}}$ ($\text{SN}^{\text{YFa}+}$) may also contribute to the pressure response, although it is less sensitive than cPRCs and has very few synapses (Williams et al., 2017).

Another indirect observation that is consistent with cPRCs being the primary pressure receptors is that one-day-old larvae that lack differentiated cPRCs (Fischer et al., 2010) do not respond to pressure (Figure 1—figure supplement 2A).

c-opsin-1 mutants have a reduced pressure response

cPRCs express ciliary-opsin-1 (c-ops-1), which forms a UV-absorbing photopigment (Arendt et al., 2004; Tsukamoto et al., 2017; Verasztó et al., 2018). Knocking out the *c-ops-1* gene abolishes a UV-avoidance response in *Platynereis* larvae (Verasztó et al., 2018). As cPRCs respond to pressure increases, we tested whether *c-ops-1* knockout mutants ($\text{c-ops-1}^{\Delta 8/\Delta 8}$) also showed a defect in the pressure response.

A range of step increases in pressure were applied to single batches of either wild-type (WT) or $\text{c-ops-1}^{\Delta 8/\Delta 8}$ three-day-old larvae (Figure 3—figure supplement 1A). The assays were carried out in a smaller pressure vessel (height: ~4 cm), to allow consistent imaging of the fewer mutant larvae available. The swimming speed of $\text{c-ops-1}^{\Delta 8/\Delta 8}$ mutant larvae was not significantly different from WT larvae ($p = 0.118$, unpaired Wilcoxon test for lower speed in mutants; Figure 3—figure supplement 1B). $\text{c-ops-1}^{\Delta 8/\Delta 8}$ larvae

173 responded in a graded manner to increases in pressure by upward swimming (Figure 3A; Figure 3—
174 figure supplement 1C). However, their response was weaker than the response of age-matched *WT*
175 larvae (Figure 3—figure supplement 1C). An ANOVA comparison showed that a model considering the
176 genotype better explained the data than a model without this variable, for either a simple or a polynomial
177 linear regression model (p-values = 9.98e□□□ and 9.92e□□□, respectively). Ciliary beating prior to
178 pressure increase was not significantly different between *c-ops-1*^{Δ8/Δ8} and *WT* larvae ($p = 0.835$, unpaired
179 Wilcoxon test for lower CBF in mutants; Figure 3—figure supplement 1D). Upon pressure increases, CBF
180 in *c-ops-1*^{Δ8/Δ8} larvae showed a significant increase to the three highest pressure levels tested (237.5 mb
181 p = 0.014, 556 mb p = 9.7 E-05, 988 mb p = 6.35 E-05; one-tailed paired t-test with Bonferroni correction
182 testing for an increase in CBF; Figure 3B). *c-ops-1*^{Δ8/Δ8} larvae also showed significant increases in max.
183 Δ%CBF as the pressure stimulus was increased (Figure 3—figure supplement 1E; compare to the *WT*
184 data in Figure 3B), with no significant difference in the increase to *WT* larvae (Figure 3—figure supplement
185 1F). In summary, *c-ops-1*^{Δ8/Δ8} larvae can still respond to changes in pressure in a graded manner, but
186 the response is weaker than in *WT* larvae, both at the population and at the single-larva levels. This
187 indicates that c-opsin-1 is not directly required for the pressure response, but its absence leads to a
188 weakened response to pressure.

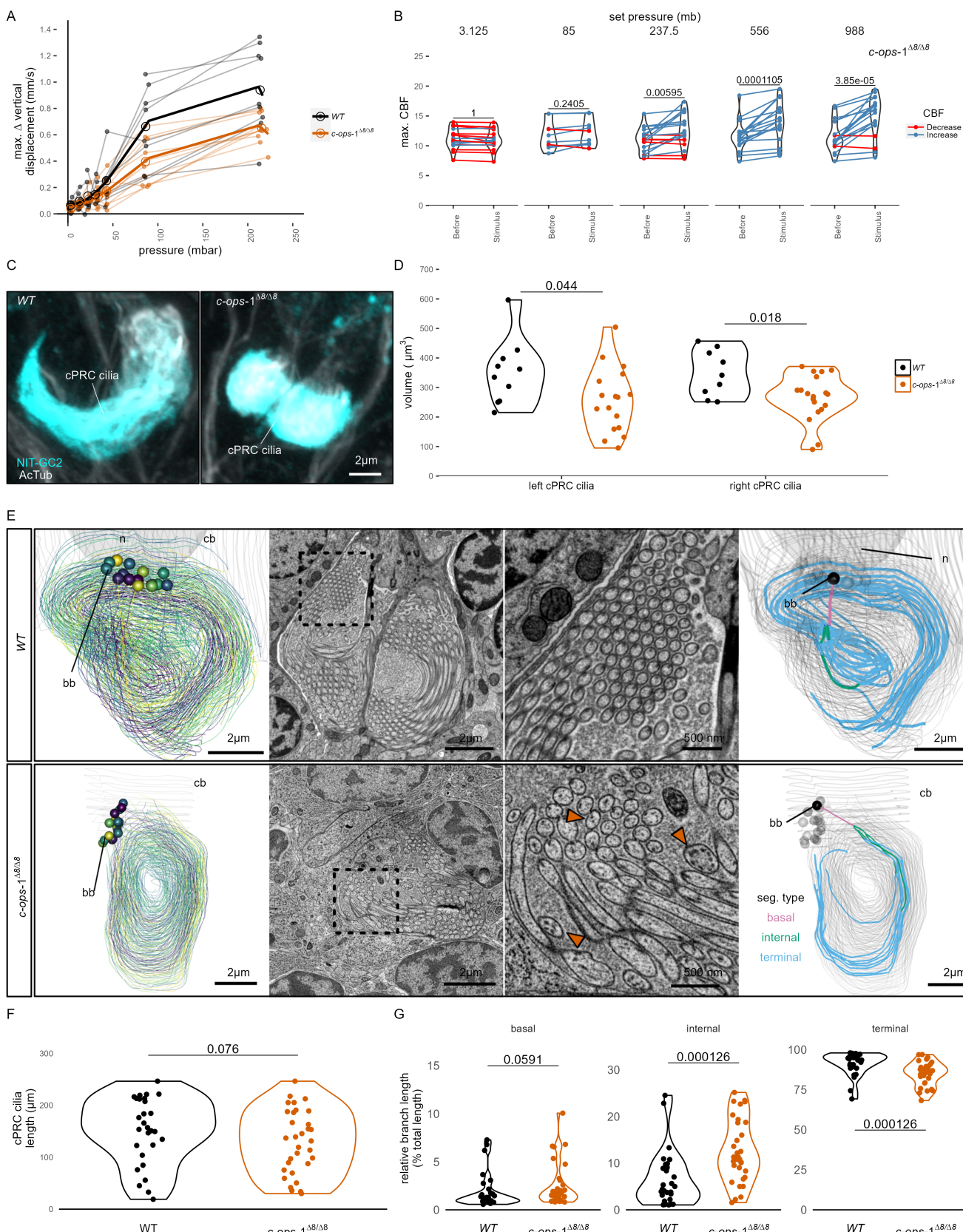


Fig. 3: Figure 3. $c\text{-ops-1}^{\Delta 8/\Delta 8}$ larvae show a weaker response to pressure and have structural defects in cPRC cilia. (A) Maximum change in vertical displacement of WT and $c\text{-ops-1}^{\Delta 8/\Delta 8}$ three-day-old larvae for each pressure step-change tested. Data points from the same batch are joined by lines. Larger open circles indicate the mean value. Thicker solid lines show the regression model predictions. N=7-9 ($c\text{-ops-1}^{\Delta 8/\Delta 8}$), N=8-10 (WT) batches. (B) Max. CBF that individual $c\text{-ops-1}^{\Delta 8/\Delta 8}$ larvae reached in the 30 s prior (Before), or during the first 30 s of the indicated increase in pressure (Stimulus). Data points from the same larva are joined by lines. Colored lines indicate data with P < 0.05 in comparison to baseline.

189 **c-opsin-1 mutants have defects in cPRC cilia**

190 The reduced response of *c-ops-1^{Δ8/Δ8}* larvae to pressure may stem from morphological defects of the
191 cPRC sensory cilia in these mutants. We used stainings with acetylated tubulin and NIT-GC2, an antibody
192 specifically marking cPRC cilia (see Figure 2D) to measure the volume of the ciliary compartment in *WT*
193 and *c-ops-1^{Δ8/Δ8}* larvae (Figure 3C; Figure 3—figure supplement 1G). Volumetric imaging in two-day-old
194 larvae stained with these antibodies revealed that the cPRC ciliary compartment in *c-ops-1^{Δ8/Δ8}* larvae
195 was significantly smaller than in age-matched *WT* larvae ($p = 0.044$ and 0.018 for left and right ciliary
196 compartments, one-tailed unpaired t-test with Bonferroni correction; Figure 3D). In some cases, cPRC
197 ciliary compartments were drastically reduced, albeit never completely absent in all four cells (Figure 3—
198 figure supplement 1F). A reduced ciliary compartment may underlie the weaker responses of *c-ops-1^{Δ8/Δ8}*
199 larvae to pressure.

200 To further investigate the morphological defects of cPRC sensory cilia in *c-ops-1^{Δ8/Δ8}* larvae, we recon-
201 structed the cPRC ciliary structure of a mutant larva using volume electron microscopy. We compared
202 this reconstruction to a volume EM dataset of cPRC cilia from a three-day-old *WT* larva previously
203 reported (Verasztó et al., 2018). The two *WT* cPRCs reconstructed have 14 to 15 ramified cilia tightly
204 wrapped on themselves (Figure 3E, top row, Video 6). Branching occurs close to the basal body, soon
205 after cilia protrude from the cell body. Most branches inherit an individual microtubule doublet. The
206 15 to 17 cilia of the two cPRCs reconstructed in a *c-ops-1^{Δ8/Δ8}* larva revealed a more sparsely packed
207 structure (Figure 3E, bottom row; Figure 3—figure supplement 1A, Video 7). Mutant cilia are not signifi-
208 cantly shorter than *WT* cPRC cilia ($p = 0.076$, Wilcoxon test for longer *WT* cilia, Figure 3F). However, we
209 noticed when comparing cross-sections of each genotype that individual branches of mutant cPRC cilia
210 often contained more than one microtubule doublet (arrowheads in Figure 3E; Figure 3—figure supple-
211 ment 2A). This suggests that cPRC cilia of *c-ops-1^{Δ8/Δ8}* larvae have alterations in branching morphology.
212 We indeed found that the terminal branches of cilia in the mutant are significantly shorter ($p = 1.26 \times 10^{-4}$
213 Wilcoxon test for shorter branches in the mutant, Figure 3G, right-most plot), while internal branches are
214 longer than those in the *WT* ($p = 1.26 \times 10^{-4}$; Wilcoxon test for longer branches in the mutant, Figure 3G,
215 middle plot). Basal branches also tended to be larger, but no statistically significance can be concluded
216 ($p = 0.06$, Wilcoxon test for longer branches in the mutant, Figure 3G, left-most plot). This result sup-
217 ports the former observation that branching occurs more distally to the basal body in *c-ops-1^{Δ8/Δ8}* larvae.
218 Longer internal branches in mutant cPRC cilia would also explain the presence of ciliary profiles with
219 more than one microtubule doublet (Figure 3—figure supplement 2A).

220 Overall, our physiological and genetic analyses suggest that the brain cPRCs act as graded and fast-
221 adapting pressure receptors. In *c-ops-1^{Δ8/Δ8}* larvae, the ciliary compartment is smaller and shows mor-
222 phological defects, revealing a genetic requirement for c-opsin-1 in the establishment of the sensory
223 compartment and supporting the idea that the cPRC ciliary compartment is the site of pressure transduc-
224 tion.

225 **Synaptic transmission from serotonergic ciliomotor neurons mediates pressure-induced**
226 **increases in ciliary beating**

227 The complete synaptic wiring diagram of the cPRCs was previously reported from an electron microscopy
228 volume of a three-day-old larva (Figure 4A-B; Verasztó et al. (2018)). The shortest neuronal path from
229 cPRCs to the prototroch involves a feed-forward loop from the cPRCs to two types of postsynaptic in-
230 terneurons, the INNOS and the INRGWa cells (Figure 4B). INRGWa cells in turn synapse on a pair of
231 head serotonergic ciliomotor neurons (Ser-h1). Ser-h1 cells directly innervate the prototroch ciliary band
232 and synapse on the MC head cholinergic ciliomotor neuron (Figure 4B). Ser-h1 cells are thought to pro-
233 mote ciliary beating by directly releasing serotonin onto the ciliary band cells and indirectly by inhibiting
234 the cholinergic MC neuron that is required to arrest ciliary beating (Verasztó et al., 2017).

235 To directly test the involvement of the Ser-h1 cells in the pressure response, we used a genetic strat-
236 egy to inhibit synaptic release from serotonergic neurons. We used transient transgenesis to drive the
237 expression of the synaptic inhibitor tetanus-toxin light chain (TeTxLC) (Sweeney et al., 1995) under the
238 promoter of *tryptophan hydroxylase (TPH)*, a marker of serotonergic neurons (Verasztó et al., 2017). The
239 *TPH* promoter labels the head Ser-h1 and other serotonergic cells including the Ser-tr1 trunk ciliomotor
240 neurons. Of the cells labelled with this promoter, only Ser-h1 is postsynaptic to cPRCs and provides
241 strong innervation to the prototroch cells and the MC cell (Verasztó et al., 2017).

242 The construct (Figure 4C) drives the expression of both TeTxLC and an HA-tagged palmitoylated td-
243 Tomato reporter, separated by P2A, a self-cleaving peptide previously used in *Platynereis* (Bezares-
244 Calderón et al., 2018). The mosaic expression of this construct resulted in the labeling of different sub-
245 sets of serotonergic neurons. We selected animals showing labelling in Ser-h1 (most larvae were also
246 labelled in Ser-tr1 and other unidentified serotonergic cells). We confirmed the expression of the trans-
247 gene in Ser-h1 by immunostaining against the HA-tag of Palmi-tdTomato (Figure 4D). Larvae expressing
248 TeTxLC in Ser-h1 showed an increase in CBF only at the highest pressure used (988 mb p = 0.004;
249 one-tailed paired t-test with Bonferroni correction testing for an increase in CBF; Figure 4E, bottom row).
250 Larvae injected with a control plasmid expressing only Palmi-tdTomato but not TeTxLC in Ser-h1 (Figure
251 4C) showed a significant increase in CBF at the three highest pressure levels applied (237.5 mb p =
252 0.023, 556 mb p = 0.009, 988 mb p = 0.004; one-tailed paired t-test with Bonferroni correction testing for
253 an increase in CBF; Figure 4E, top row; Figure 4—figure supplement 1A). The metric max. Δ%CBF was
254 not significantly different between control and TeTxLC-injected larvae (Figure 4—figure supplement 1B).
255 These results indicate that TeTxLC-mediated inhibition of Ser-h1—albeit incomplete and in most cases
256 limited to one of the two cells—leads to a noticeable dampening of the pressure response at the level of
257 the ciliary band. This suggests that synaptic release from serotonergic neurons is required to increase
258 ciliary beating upon pressure increase. Our data support the model that Ser-h1 neurons, and no other
259 serotonergic cells, are specifically required for this response, because this cell type was labelled in all
260 animals tested and these cells directly innervate the prototroch.

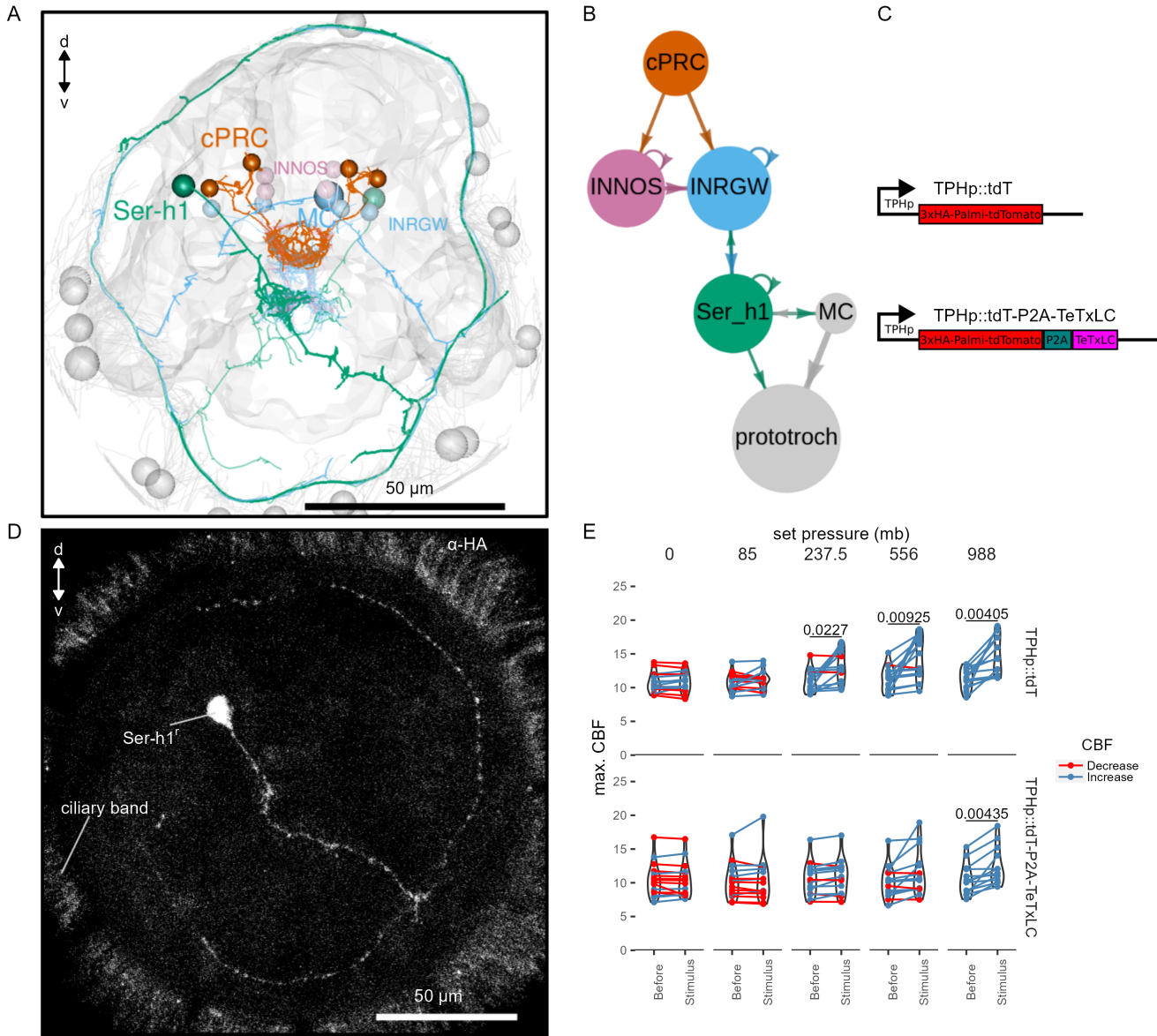


Fig. 4: Figure 4. TeTxLC expression in Ser-h1 neurons inhibits CBF increase during pressure. (A-B) Volume EM reconstruction (A) of the cells in the cPRC synaptic circuit (B). cPRCs synapse in the middle of the brain on both INNOS and INRGWa neurons. INRGWa cells synapse on Ser-h1 neurons, which directly innervate the ciliary band and also target the MC cell. Only the cells in the shortest path to the prototroch are included. (C) Schematic of the gene constructs used to test the role of Ser-h1 in the pressure response. The TPHp::tdT construct drives expression of the reporter protein Palmi-tdTomato in Ser-h1 and other serotonergic neurons. It was used as a control. The TPHp::tdT-P2A-TeTxLC construct expresses Palmi-tdTomato and the synaptic blocker TeTxLC as a fusion that gets post-translationally self-cleaved by the P2A peptide. (D) Maximum intensity projections of a larva injected with the TPHp::tdT-P2A-TeTxLC construct and stained with α -HA. Ser-h1 was labelled in this animal. Anterior view. (E) Max. CBF that single larvae reached in the 30 s prior (*Before*), or during the first 30 s of the indicated increase in pressure (*Stimulus*). Data points for the same larva are joined by lines. Larvae were injected either with the control plasmid TPHp::tdT (top row, N = 14-16 larvae), or with the TPHp::tdT-P2A-TeTxLC plasmid (bottom row, N = 13-16 larvae). One-tailed paired t-test with Bonferroni correction testing for an increase in CBF; p-values < 0.05 are shown. Figure 4—source data 1 (E).

261 **Discussion**

262 This work provides insights into the neuronal mechanisms of pressure sensation and response in a ma-
263 rine planktonic larva. Our findings suggest that increases in pressure, either due to the larva's own
264 actions (sinking or diving) or to downwelling currents, lead to the activation of the sensory cPRCs (Fig-
265 ure 5). The activation is proportional to the magnitude of pressure change and leads to the activation of
266 the downstream circuit that converges onto the Ser-h1 neurons and ultimately leads to increased ciliary
267 beating. The Ser-h1 cells could secrete serotonin (5-HT) onto the ciliary band, which from pharmaco-
268 logical assays is known to increase ciliary beat frequency (Verasztó et al., 2017). Ser-h1 neurons may
269 simultaneously inhibit the cholinergic ciliomotoneuron MC neuron (Verasztó et al., 2017), thereby pre-
270 venting ciliary arrests while the larva tries to compensate for the increased pressure. Upon a decrease
271 in pressure, three-day-old (but not two-day-old) larvae also show an off-response characterised by down-
272 ward swimming. We have not analysed in detail the neuronal mechanisms of this response but it may
273 depend on an inverted activation of the cPRC circuit, as happens during UV avoidance (Jokura et al.,
274 2023). Pressure 'on' and pressure 'off' thus induce behavioural responses with opposite sign such that
275 larvae move to compensate for the pressure change. The response is directional along the pressure
276 gradient (even if larvae do not detect the gradient but temporal changes) and we refer to it as barotaxis.

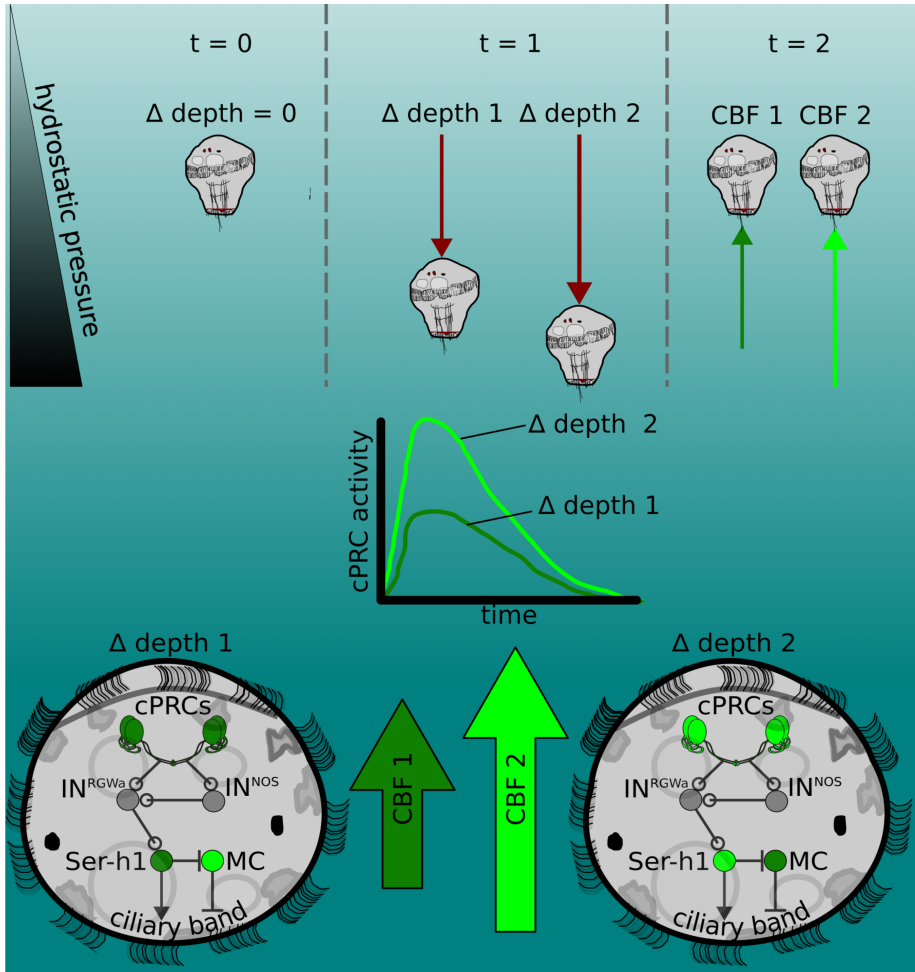


Fig. 5: Figure 5. The pressure response as a depth-retention mechanism mediated by the ciliary photoreceptor-cell circuit. (Top) *Platynereis* larvae maintain their position in the water column by controlling the beating dynamics of the ciliary band ($t = 0$, no net change in depth, $\Delta \text{depth} = 0$). A sufficiently rapid increase in depth (at $t = 1$) caused by intrinsic or extrinsic factors would lead to an increase in hydrostatic pressure. The change in depth relative to the previous state ($\Delta \text{depth} 1$ or $\Delta \text{depth} 2$) will be perceived by the larva, which will try to counteract this change by increasing ciliary beat frequency of the prototroch, leading to upward swimming (at $t = 2$) until the pressure returns to the level previously experienced. A smaller change in pressure ($\Delta \text{depth} 1$) will lead to a smaller increase in CBF (CBF 1, light green arrow) than a larger change (CBF 2). (Middle) Changes in pressure are sensed by the cPRCs. These sensory cells are activated in a graded manner according to the change in pressure. (Bottom) cPRCs signal via a postsynaptic circuit including the INRGWa and INNOS interneurons to the Ser-h1 neurons. Activation of these serotonergic neurons is required to increase ciliary beating directly on the prototroch cells and indirectly by inhibiting the MC neuron (CBF 1 or CBF2) proportional to the change in pressure.

277 Our proposed depth-retention model complements a previously reported spectral depth-gauge mecha-
 278 nism in the *Platynereis* larva based on its ability to respond to UV and green light (Verasztó et al., 2018).
 279 As previously hypothesized for other planktonic larvae (Sulkin, 1984), pressure sensing in *Platynereis*
 280 may operate through negative feedback to retain a particular depth, while light as a more variable stim-
 281 ulus could drive intensity and wavelength-dependent changes in the vertical position of larvae. In future,

282 it will be interesting to explore how responses to pressure and to directional (Randel et al., 2014) and
283 non-directional light cues (Verasztó et al., 2018) across wavelengths and intensities interact to guide
284 larval swimming.

285 Our unexpected finding that ciliary photoreceptors, previously shown to be sensitive to UV and green
286 light (Verasztó et al., 2018), are also activated by pressure increase suggests that the integration of light
287 and pressure could begin at the sensory level in a single cell type. UV light activates the cPRCs to
288 induce downward swimming while pressure increases induce upward swimming. The calcium dynamics
289 of cPRCs depends on the stimulus applied and may therefore underlie the mechanism by which the
290 cells decode and transmit a sensory signal to the downstream circuit. UV induces a transient increase
291 and subsequent drop in Ca^{2+} levels followed by a sharp NO-dependent increase that persists even
292 after UV stimulation ends (Jokura et al., 2023). In contrast, pressure induces a transient increase in
293 Ca^{2+} levels that terminates with the stimulus. These observations suggest that the integration of light
294 and mechanical cues already occurs at the sensory-cell level. The different activation dynamics may
295 lead to the release of different neurotransmitter and neuromodulator cocktails (cPRCs are cholinergic,
296 GABAergic, adrenergic and peptidergic (Jokura et al., 2023; Randel et al., 2014; Tessmar-Raible et al.,
297 2007; Williams et al., 2017)) and different activation patterns in the postsynaptic cells. Similar integration
298 can occur in *Drosophila* larvae, where UV/blue light and noxious mechanical stimuli are detected by the
299 same sensory neuron that together with other cells converges onto a circuit processing multisensory
300 stimuli (Imambocus et al., 2022). In *Platynereis*, other sensory cells (e.g., the $\text{SN}^{\text{d1_unp}}$ cells; Figure
301 2—figure supplement 1) may contribute to distinguishing the nature of the stimulus.

302 The cellular and molecular mechanisms by which cPRCs sense and transduce changes in hydrostatic
303 pressure deserve further enquiry. The mechanism may involve the differential compression of micro-
304 tubules along each ciliary branch (Li et al., 2022; Nasrin et al., 2021), or differential displacement of
305 fluid inside the cilium (Bell, 2008). The cPRCs have a unique multiciliated structure and are embedded
306 in a protected environment different from fluid-exposed cilia such as hydrodynamic mechanosensory
307 cilia (Bezares-Calderón et al., 2018). These features are hard to reconcile with current models of ciliary
308 mechanosensation (e.g., see review by R. Ferreira et al. (2019)). Instead, the mechanism of pressure
309 sensation at work in cPRCs may share more similarities with non-neuronal cells detecting pressure, such
310 as chondrocytes (Pattappa et al., 2019) and trabecular meshwork cells (Luo et al., 2014).

311 The molecular mechanisms of pressure detection remain unclear. Components of the phototransduction
312 cascade may be involved in pressure sensation. Our results indicate that the ciliary opsin required for
313 detecting UV light is not essential for pressure sensation. This molecule rather indirectly affects the
314 ability of cPRCs to sense pressure by contributing to the development or maintenance of a ramified
315 ciliary sensory structure. The structural role of opsins for shaping ciliary cell morphology has also been
316 reported in other photoreceptor and mechanoreceptor cells (Lem et al., 1999; Zanini et al., 2018). The
317 direct transducer of pressure may be a TRP channel. TRP channels can signal downstream of opsins in
318 phototransduction cascades and have been postulated as the ultimate integrators of sensory stimuli (Liu
319 and Montell, 2015). Mechanosensitivity has also recently been reported for vertebrate rods (Bocchero
320 et al., 2020), including the activation of these ciliary photoreceptors by pressure (Pang et al., 2021). The
321 cellular and molecular mechanisms behind this sensitivity are still unclear, but TRP or Piezo channels